DIVERGENCE OF SWEPT WINGS

By Franklin W. Diederich and Bernard Budiansky

Langley Memorial Aeronautical Laboratory
Langley Field, Va.

ADVANCE COPY

TRANSMITTED ON   JUL 7 1948

20000807 143

April 1948

DTIC QUALITY INSPECTED 4

NATIONAL ADVISORY COMMITTEE FOR AERONAUTICS

DIVERGENCE OF SWEPT WINGS

By Franklin W. Diederich and Bernard Budiansky

SUMMARY

An analysis of the divergence of swept untapered and tapered wings
with stiffnesses varying as the fourth power of the chord has been
performed and checked experimentally. The results are presented in a
set of charts and approximate formulas suitable for quick estimates of
the divergence dynamic pressure and hence the divergence speed.

.These results indicate that the divergence speed drops rapidly
as sweepforward increases to about 40° but that wings with moderate or
large sweepback cannot diverge. The location of the elastic axis is
found to affect the divergence speed most at low angles of sweep, where
movement of the elastic axis forward (or the aerodynamic center aft)
raises the divergence speed. The effect of wing taper is to increase
the divergence speed of essentially unswept wings and to decrease the
divergence speed of wings with moderate and large angles of sweep in
the case of the prescribed stiffness variation. Evidence is presented
to indicate that these effects may not be observed for actual stiffness
variations, in which cases a more refined analysis must be resorted to.

INTRODUCTION

The emphasis on the use of sweptback or sweptforward wings for
high-speed flight has created widespread interest in the aeroelastic
behavior of swept wings. The present paper is concerned with the
theoretical determination of one of the most fundamental aeroelastic
parameters, the wing divergence speed.

The divergence of wings or tail surfaces is an instability
phenomenon which results from the interaction of aerodynamic and
structural forces. If a wing or tail is given a deflection of
arbitrary magnitude, the aerodynamic forces often act in such a way
as to increase the given deflection, whereas the structural forces
always tend to decrease the deflection. Since the aerodynamic forces
increase with the flying speed, whereas the structural forces are
independent of it, a speed will often exist at which the two sets of
forces are exactly in balance, so that they tend to maintain the given
deflection. This speed is known as the divergence speed, since any
further increase in speed causes the aerodynamic forces to predominate
over the restraining structural forces and tends to increase any
deformation until structural failure occurs.

The theory of divergence of unswept wings has reached a considerable degree of refinement. Since H. Reissner's original analysis of the problem (reference 1), a great deal of material has been published on this subject both in the United States and in Great Britain (for instance, references 2, 3, and 4); the latest methods treat arbitrary stiffness variation (reference 2) and account for aerodynamic induction (references 3 and 4).

The analysis of the divergence of swept wings is complicated by the fact that, unlike the case of unswept wings, the air forces depend on the bending deformations as well as on the twisting deformations. A first approximation to the solution of the problem is presented in reference 5 by means of a "semirigid" approach that does not take into account spanwise variation of the wing distortion.

The present paper gives the results of a more exact analysis that considers the effect of elastic bending and twisting along the wing span. Theoretical derivations are given for the divergence speeds of swept wings with constant chord and constant flexural and torsional stiffnesses along the span, as well as for swept wings with linearly varying chords and with flexural and torsional stiffnesses varying quartically with the chord. The results of the theoretical analysis are presented in curves of nondimensional parameters from which the divergence speed can be estimated for a given design.

In order to verify the theory and establish the effects of the assumptions involved, a limited number of tests were made in the Langley 4.5-foot flutter research tunnel on models of constant chord and stiffness at low Mach numbers. The results of these tests are presented and are compared with the theory.

SYMBOLS

A	aspect ratio	$\left(\dfrac{\text{Span}^2}{\text{Total area}}\right)$
a	dimensionless parameter	$\left(\dfrac{q \cos^2\Lambda\, m_e e_1 c_r^2 L^2}{(GJ)_r}\right)$
a_D	value of parameter a at divergence	
d	dimensionless parameter	$\left(\dfrac{q \cos^2\Lambda\, m_e c_r L^3 \tan\Lambda}{(EI)_r}\right)$
d_D	value of parameter d at divergence	
c	chord, measured perpendicular to elastic axis, feet	

c_r chord at effective root (fig. 1), feet

c_t effective chord at tip (fig. 1), feet

EI effective bending stiffness in planes perpendicular to elastic axis, pound-feet^2

$(EI)_r$ bending stiffness at effective root, pound-feet^2

e_1 distance from elastic axis to aerodynamic center (positive forward), fraction of chord

GJ effective torsional stiffness in planes perpendicular to elastic axis, pound-feet^2

$(GJ)_r$ torsional stiffness at effective root, pound-feet^2

k chord ratio, c/c_r

K_1, K_2 constants

l running air load along elastic axis, pounds per foot

L length of one wing along elastic axis (see fig. 1), feet

M free-stream Mach number

M_{cr} critical Mach number of section perpendicular to elastic axis

m_0 section lift-curve slope, per radian

m_e effective section lift-curve slope, per radian

q dynamic pressure, pounds per square foot $\left(\frac{\rho}{2}V^2\right)$

q_D dynamic pressure at divergence, pounds per square foot $\left(\frac{\rho}{2}V_D^2\right)$

V free-stream velocity, feet per second

V_D free-stream velocity at divergence, feet per second

V_Λ component of free-stream velocity normal to elastic axis, feet per second

y distance along elastic axis (see fig. 1), feet

4

α_e effective angle of attack of a section perpendicular to elastic axis, radians

η semispan position along elastic axis (y/L)

Γ local dihedral angle, radians, or slope of wing deflection curve at elastic axis (see fig. 1)

Λ angle of sweep measured to elastic axis, positive for sweepback, degrees

λ taper ratio (c_t/c_r)

ρ density of air stream, slugs per cubic foot

φ angle of twist in a plane perpendicular to elastic axis, radians

THEORETICAL RESULTS

Untapered Swept Wings

A theoretical analysis of the divergence of a swept wing of uniform chord (fig. 1(a)) and stiffness is contained in the appendix. The analysis involves the following limitations and assumptions:

(a) Aerodynamic induction is taken into account only insofar as an over-all correction is applied to strip theory

(b) Aerodynamic as well as elastic forces are based on the assumption of small deflections

(c) The wing is clamped at the root perpendicular to a straight elastic axis (see fig. 1(a)), and all deformations are given by the elementary theories of bending and of torsion about the elastic axis.

Within the limitations of these assumptions an exact theoretical solution for the divergence speed is obtained. The solution consists of a relationship between two nondimensional parameters,

$$a_D = \frac{q_D \cos^2\Lambda\, m_e e_1 c_r^2 L^2}{(GJ)_r} \tag{1}$$

and

$$d_D = \frac{q_D \cos^2\Lambda m_e c_r L^3 \tan \Lambda}{(EI)_r} \qquad (2)$$

which is presented in figure 2.

It is seen that the ratio of these parameters

$$\frac{d_D}{a_D} = \left[\frac{(GJ)_r}{(EI)_r}\right]\left[\frac{L}{e_1 c_r}\right] \tan \Lambda \qquad (3)$$

depends only on the known geometrical and physical parameters of the problem. Thus, from the theoretical plot of a_D against d_D/a_D shown in figure 3, the divergence speed can be obtained for any particular uniform wing. In order to cover the entire range of values of the independent parameter, it is convenient to plot d_D against a_D/d_D for large positive and negative values of d_D/a_D.

Tapered Swept Wings

A theoretical solution for the divergence speed of linearly tapered swept wings (see fig. 1(b)) has also been effected in the appendix. The assumptions listed in the foregoing section apply to this case as well. The bending and torsional stiffnesses are assumed to vary as the fourth power of the chord; this variation is realized for a wing having geometrically similar cross sections, such as a solid wing or one all structural dimensions of which are proportional to the local chord.

Theoretical curves similar to those of figure 3, relating the nondimensional parameters a_D and d_D, have been computed for swept wings having taper ratios λ of 0.2, 0.5, and 1.5. The various branches of these curves, together with those for the uniform wing (taper ratio 1.0) are, for convenience, given separately in figure 4(a), 4(b), and 4(c).

Effective Lift-Curve Slope

In the calculations of the lift acting on the individual wing sections, it has been assumed that the aerodynamic interaction of the sections may be neglected if an over-all span correction is made to the section lift-curve slope. Thus, the value of m_e to be used is the two-dimensional value m_0

6

for sections normal to the elastic axis multiplied by a suitable correction factor. In reference 2, Shornick, in computing the divergence speed of unswept wings by strip theory, applies the aspect-ratio correction

$$m_e = m_o \frac{\frac{A}{2}}{\frac{A}{2} + 2} \tag{4}$$

For the case of an unswept uniform wing with $\frac{A}{2} = 3.14$, this assumption yields a divergence speed that differs by less than 1 percent from the result calculated by Hildebrand and Reissner (reference 3) by lifting-line theory. (The parameter β calculated by lifting-line theory in reference 3 may be compared directly with $\sqrt{a_D} \sqrt{\frac{m_o}{m_e}}$ of the present paper.)

Equation (4) may be extended to swept wings by means of the reasoning used in reference 6. If the air forces are considered to act in planes perpendicular to the elastic axis instead of parallel to the plane of symmetry, the following relation is obtained

$$m_e = m_o \frac{A}{A + 4 \cos \Lambda} \tag{4a}$$

This approximation for finite-span effect may be used for subsonic and subcritical Mach numbers. For supersonic and supercritical Mach numbers, it is inapplicable; no span correction is available at present for these speed ranges. Neglect of the finite-span effects, however, will always tend to give conservative results.

Location of the Effective Root

If the results of the preceding analysis are applied to an actual wing, it is necessary to assume that the wing is clamped along a line perpendicular to the elastic axis. From the data and the analysis presented in reference 7 it appears that the amount of wing twist can be estimated closely by assuming the wing to be clamped at a line through the intersection of the elastic axis and the side of the fuselage, if the carry-through structure is fairly rigid.

The bending deflections are estimated in reference 7 by considering the wing supported flexibly at a line through the innermost point of the trailing edge (in the case of a sweptback wing) or of the leading edge (in the case of a sweptforward wing). This effect may be taken into account in the preceding analysis by modifying the root boundary conditions. If the carry-through structure is fairly rigid the resulting divergence speed is the same, for all practical purposes, as the value obtained by

considering the wing mounted rigidly at a line through the intersection of the elastic axis and the side of the fuselage. This line is consequently considered the effective root of an actual wing, as shown in figure 1(c).

APPLICATION OF THE THEORETICAL RESULTS

Selection of the Aerodynamic Parameters

Both the section lift–curve slope m_0 and the aerodynamic center (and consequently the distance from the aerodynamic center to the elastic axis, e_1) vary with Mach number and, in the transonic range at least, with the angle of attack. The parameters should be chosen at the angle of attack near the design value which yields the most conservative results. The choice of the Mach number depends on the purpose for which the divergence speed or dynamic pressure is calculated.

If the divergence speed is calculated for its own sake, the parameters should be chosen at the Mach number corresponding to the divergence speed; resort to a trial and error procedure may therefore be necessary. If, on the other hand, it is desired to calculate the divergence speed or dynamic pressure as a reference value for one of the other aeroelastic phenomena, the aerodynamic parameters should be chosen at the Mach number of interest for the particular phenomenon. The dynamic pressure calculated in this manner will not usually be the true value but appears to be the divergence value only at the given Mach number and will vary with Mach number. If the variation of this reference divergence dynamic pressure q_D is plotted against Mach number and the actual dynamic pressure q is plotted on the same graph, the intersections of the two lines will determine the true values of the divergence Mach number and dynamic pressure; this procedure therefore constitutes another way of calculating the divergence speed. Such a plot is shown in figure 5 for a straight and a sweptforward wing designed for high–speed flight.

The values of the aerodynamic parameters are best obtained from experimental section data for the lift and pitching moment of the given section at the Mach number of interest. If such data are not available, the section lift–curve slope m_0 may be approximated by the Glauert–Prandtl and Ackeret relations in the subsonic and supersonic regions, respectively, and by an arbitrary constant value which depends on the critical Mach number in the transonic region, as indicated in figure 6. The aerodynamic center is located near the quarter–chord point at subsonic speeds and at 40 to 45 percent of the chord at supersonic speeds. Its location at transonic speeds is not well established; it may move forward of the quarter–chord point, however, before receding to the supersonic position.

Use of the Curves

The aerodynamic parameters are selected for a given Mach number and the section lift-curve slope is corrected for finite span effects in the manner previously indicated. With these parameters and the given geometric parameters the ratio d_D/a_D may be determined from equation (3). The value of a_D or d_D is then obtained from figure 4 and the divergence dynamic pressure calculated from either of the two following relations:

$$q_D = a_D \frac{(GJ)_r}{m_e c_r L^3 \cos^2 \Lambda} \frac{L}{e_1 c_r} \tag{5}$$

$$= d_D \frac{(EI)_r}{m_e c_r L^3 \cos^2 \Lambda} \cot \Lambda \tag{5a}$$

The divergence speed is given by the relation

$$V_D = \sqrt{\frac{q_D}{\rho/2}} \tag{6}$$

If the value of q_D as calculated in this manner is negative the wing cannot diverge, since a negative dynamic pressure does not correspond to any real speed. A negative value, however, is still useful as a reference value.

Unless the wing under consideration is solid or has geometrically similar cross sections along the span, it must be kept in mind that the actual divergence speed or dynamic pressure may be below that calculated by this method for reasons cited subsequently in the "DISCUSSION."

Use of Approximate Formulas

The relation between the values a_D and d_D may be approximated closely by a straight line. The agreement between the exact curves and curves representing the linear relation is seen in figures 2 and 3 in the case of a uniform wing. From the linear approximation an expression for the divergence dynamic pressure may be obtained of the following form:

$$q_D = \frac{(GJ)_r}{m_e c_r L^3 \cos^2 \Lambda} \left(\frac{L}{e_1 c_r}\right) \left[\frac{K_1}{1 - K_2 \frac{(GJ)_r}{(EI)_r}\left(\frac{L}{e_1 c_r}\right)\tan \Lambda}\right] \tag{7}$$

where the constants K_1 and K_2 are given in the following table:

λ	K_1	K_2
0.2	2.81	0.614
.5	2.74	.497
1.0	2.47	.390
1.5	2.22	.326

Equation (7) may be used with almost the same accuracy as the curves of figure 4. This equation should be particularly convenient for calculating the stiffnesses required for a given value of the dynamic pressure at divergence.

EXPERIMENTAL RESULTS

As a check on the theory several divergence tests on uniform swept wings were made in the Langley 4.5-foot flutter research tunnel. In the first series of tests a thin plate of 24S-T aluminum alloy, 5 inches by 30 inches by 0.126 inch, was held in the tunnel essentially as shown in figure 1(a); the angle of sweep was varied by means of the rotating root fixture. The experimental divergence dynamic pressure was taken to be the highest value at which the wing would remain in an undeflected position when the root section was at zero angle of attack relative to the true air stream. From the experimental data obtained, shown in table I, the divergence dynamic pressure is plotted against the angle of sweep in figure 7(a). The variation of divergence dynamic pressure with sweep obtained from the theory of the present paper is also shown in figure 7(a). No experimental data have been obtained for sweepback; the wing fluttered, rather than diverged, at zero sweep, and flutter would undoubtedly be critical at any angle of sweepback. However, the agreement between the present theory and experiment for angles of sweepforward up to 40° is excellent.

A similar series of tests was run for another rectangular aluminum wing, 4 inches by 24 inches by 0.0977 inch. (See table I.) The results given in figure 7(b) also show good agreement between theory and experiment.

A third series of tests was run on flat-plate aluminum models, 5 inches by 30 inches by 0.125 inch, that were not rectangular, but were clamped at the root, and cut at the tip parallel to the wind stream (fig. 1(c)). A separate model was used for each angle of sweep, but the length along the leading edge was held constant at 30 inches. These wing plan forms do not correspond to those assumed for the theory, but they do represent more closely conventional swept-wing plan forms. The experimental results are presented in table I and plotted in figure 7(c). The theoretical variation of the divergence dynamic pressure with sweep

obtained by using the effective root discussed previously (root A of fig. 7(c)) is shown by the solid-line curve. The variation obtained from theory if the effective root is considered to be at the line through the innermost point of the leading edge (root B of fig. 7(c)) is shown by the dash-line curve. It appears that the use of root A yields conservative results for all sweep angles of practical concern, but that the results obtained by using root B are on the average in somewhat better agreement with the test data for low and medium angles of sweepforward.

The curves of figure 7 are based on calculated values of $(GJ)_r$ and $(EI)_r$. The section aerodynamic center was assumed to be at the $c/4$ point, so that e_1 is 0.25. A section lift slope of 2π was assumed and corrected for span effects as shown in equation (4a). Compressibility effects were neglected in all comparisons, since the test Mach numbers were too low to warrant a correction.

DISCUSSION

The aerodynamic and structural assumptions made impose limitations on the accuracy of the analysis. The aerodynamic assumptions are concerned with the magnitude of the deflections involved as well as the treatment of the aerodynamic induction and compressibility effects. The assumption of small deflections made in obtaining the effective velocity component V_Λ (see appendix, equation (A5a)) yields results which are too low at high angles of sweep. The air forces are consequently underestimated and the divergence speed is overestimated. The correction for aerodynamic induction is only approximate; it is simple to make, however, and yields good experimental agreement. For most airplanes the divergence speed lies in the transonic or supersonic region, where the induction effects are greatly diminished, so that no correction need ordinarily be applied. The manner in which compressibility is taken into account in the analysis has not been checked experimentally and is consequently somewhat uncertain.

The location of the aerodynamic center may not be known very accurately; fortunately, however, the divergence speed of a swept wing is not very sensitive to the aerodynamic-center location at large angles of sweep, as may be seen from figure 4(c). The change in d_D, and hence the change in divergence speed, will be found to be fairly small even for rather large changes in the value of e_1 produced by changes in the aerodynamic-center location or elastic-axis location. At low angles of sweep the effect of the location of the aerodynamic center relative to the elastic axis is much more pronounced; movement of the elastic axis forward or the aerodynamic center rearward will tend to raise the divergence speed. If the aerodynamic center is behind the elastic axis, negative values will usually be obtained for the dynamic pressure at divergence, so that divergence will be impossible.

The most important of the structural assumptions involves the existence of a straight elastic axis, which permits bending and torsion to be treated independently. This assumption appears warranted in most cases. Although the exact location of this axis is often difficult to ascertain, only an approximate value is needed in view of the foregoing consideration, at least for large angles of sweep. Near the wing root, where the elastic-axis location is most uncertain, swept wings are so stiff that the location is immaterial.

The assumption of the effective root at the location indicated in figure 1(c) (root A of fig. 7(c)) leads to conservative results. This assumption appears, therefore, to be preferable to the assumption of the root at a point farther outboard, such as root B of figure 7(c). On the other hand, the assumption of the effective root B leads to results which, at least in the case of the flat-plate models tested, agree somewhat more closely with experiments for angles of sweepforward up to about 45°.

The insensitivity of the divergence speed to the relative location of the aerodynamic center and the elastic axis indicates that the effects of bending predominate at large angles of sweep (actually at large values of d_D/a_D). Even at low values of sweep, bending is quite significant; the divergence phenomenon of swept wings should therefore be referred to as "bending-torsion" divergence rather than "torsional" divergence as in the case of unswept wings.

The stiffness variation used in the analysis for tapered wings (EI and GJ vary as c^4) is realized for wings with geometrically similar cross sections; it is obtained for solid wings and closely approximates that of actual wings with a taper ratio of the order of 0.2. For higher taper ratios, actual wings are more flexible at the tip than the fourth-power variation would dictate. In order to investigate this effect, the parameter a_D has been plotted against taper ratio in figure 8 for unswept wings with stiffness variations dictated by constant bending-stress levels. The assumption has been made that the torsional stiffness is proportional to the flexural stiffness which, in turn, is based on a load distribution given by strip theory. The computations for the divergence speed were performed by a method similar to that of reference 2. Figure 8 indicates that the divergence speed of wings with this type of stiffness distribution is in general lower than that obtained for wings the stiffness of which follows the quartic variation. The divergence speed of actual wings may be expected to lie between the two curves of figure 8 and will in general be lower than that for wings the stiffness of which follows the fourth-power variation. This point must be considered when figure 4 is used; the results furnished by the curves of figure 4 may be somewhat unconservative for actual wings.

The effect of sweep may be seen from figures 3, 4, and 7. Figures 3 and 4 show that as the sweep angle (and hence the parameter d_D/a_D) is increased negatively, that is, toward increased sweepforward, the parameter a_D (and hence the divergence speed) decreases rapidly, all

other physical parameters remaining the same. Beyond a certain angle of sweepforward the $\cos \Lambda$ term in the parameter a_D becomes dominant and tends to increase the divergence speed again as seen in figure 7. Sweptback wings with a value of d_D/a_D larger than about 2 and positive values of e_1, which normally correspond to subsonic speeds, cannot diverge; nor can any sweptback or unswept wing diverge for negative values of e_1 which may exist at supersonic speeds. In either case a negative divergence dynamic pressure is obtained. This fact does not preclude the possibility of flutter in these cases, however.

The effect of taper on the divergence of swept wings of the assumed stiffness variation (GJ and EI varying as c^4) is seen from figure 4. For positive values of e_1 (subsonic case) and positive or small negative values of the sweep angle, conventional taper increases the divergence speed; for all other configurations it decreases the divergence speed. The effects of inverse taper are the opposite of those of conventional taper. These considerations must be modified in the case of actual wings, because of their deviation from the assumed stiffness distribution, so that either the curves of figure 4 must be used with some degree of conservatism or more refined analyses must be resorted to.

Although the low-speed wind-tunnel tests for divergence have been performed only on uniform wings, they serve to corroborate the theoretical analysis for uniform wings and hence, indirectly, that for tapered wings, since the assumptions are the same in either case. The rapid decrease of divergence speed with increase in sweepforward agrees with the predicted variation both qualitatively and quantitatively (up to about 40° sweepforward). This agreement indicates that the assumptions made concerning the structural and aerodynamic behavior (at low speeds) are justified. At values of sweepforward above about 40° the observed increase in divergence speed falls short of the predicted increase. This observation agrees qualitatively with the statement made previously that the analysis would tend to overestimate the divergence speed for large angles of sweep.

It is difficult to make a direct comparison with the results of the simplified approach of reference 5, but it is quite apparent that since the method of this report takes account of the spanwise variation of bending and twisting it should furnish more reliable results. If the first natural bending and torsion frequencies of a uniform cantilever beam are substituted in the expression for $\dfrac{b\omega_\alpha}{V_D}$ of reference 5, a relation may be obtained for q_D which will have both the same form as equation (7) and the same value of K_1 if a proper finite-span correction is applied; the value of K_2, however, will be 0.299 instead of 0.390, as determined by the theory of this paper for the uniform wing ($\lambda = 1.0$), so that the effect of sweep will be underestimated somewhat. This discrepancy indicates that, if the results of a semirigid analysis are applied to actual swept wings, a certain amount of caution must be exercised.

CONCLUDING REMARKS

On the basis of certain assumptions theoretical results have been obtained for the divergence of uniform and tapered wings. These results are presented in the form of charts and approximate formulas suitable for obtaining quick estimates of the divergence dynamic pressure or speed. A limited number of low-speed wind-tunnel tests on untapered models give good agreement with the theoretical results for angles of sweepforward up to 40° and appear to justify the assumptions made in the analysis. The results indicate the following conclusions:

1. The divergence speed drops rapidly as sweepforward increases up to about 40°. Wings with sweepback beyond a fairly low value cannot diverge.

2. Moving the elastic axis forward raises the divergence speed appreciably for low angles of sweep but has less effect at higher sweep angles. Wings with the elastic axis forward of the aerodynamic center (supersonic case) can only diverge for moderate or large angles of sweepforward.

3. For most practical cases, the effect of conventional taper is to increase the divergence speed of essentially unswept wings and to decrease the divergence speed of wings with moderate and large angles of sweep if the stiffness varies as the chord to the fourth power. For stiffness variations closer to the ones which are obtained for actual wings, this effect may not be observed. In order to obtain accurate results in these cases a more refined analysis must be resorted to.

Langley Memorial Aeronautical Laboratory
   National Advisory Committee for Aeronautics
      Langley Field, Va., April 16, 1948

Franklin W. Diederich
Aeronautical Research Scientist

Bernard Budiansky
Structural Engineer

Approved:
    Richard V. Rhode
   Chief of Aircraft Loads Division

Eugene E. Lundquist
Chief of Structures Research Division

epp

APPENDIX

ANALYSIS OF THE DIVERGENCE OF SWEPT WINGS

Assumptions

The analysis involves the following limitations and assumptions:

(a) Aerodynamic induction is taken into account only insofar as an over-all correction is applied to strip theory

(b) Aerodynamic as well as elastic forces are based on the assumption of small deflections

(c) The wing is clamped at the root perpendicular to a straight elastic axis (see fig. 1), and all deformations are considered to be given by the elementary theories of bending and of torsion about the elastic axis

Aerodynamic Forces

In keeping with assumptions (a) and (b), the force per unit width on a wing section in a plane perpendicular to the elastic axis resulting from bending and twisting deformations is given by

$$l = m_e \alpha_e \frac{\rho}{2} V_\Lambda^2 c \tag{A1}$$

where α_e and V_Λ are the effective angle of attack and the component of the free-stream velocity in the plane perpendicular to the elastic axis, respectively. If the free-stream velocity is resolved into three components, one along the local tangent to the elastic axis, one parallel to the chord, and one perpendicular to the other two, the effective angle of attack may be obtained as the ratio of the third component to the second and the effective velocity as the vector sum of the two components. Thus,

$$\tan \alpha_e = \frac{\sin \varphi \cos \Lambda - \cos \varphi \sin \Gamma \sin \Lambda}{\cos \varphi \cos \Lambda + \sin \varphi \sin \Gamma \sin \Lambda} \tag{A2}$$

and

$$V_\Lambda^2 = V^2 \left[(\cos \varphi \cos \Lambda + \sin \varphi \sin \Gamma \sin \Lambda)^2 + (\sin \varphi \cos \Lambda - \cos \varphi \sin \Gamma \sin \Lambda)^2 \right] \tag{A3}$$

The most convenient way of obtaining these relations is probably by use of vector analysis.

For small values of φ and Γ these relations simplify to

$$\alpha_e = \varphi - \Gamma \tan \Lambda \qquad (A4)$$

$$V_\Lambda = V \cos \Lambda \sqrt{1 + \alpha_e^2} \qquad (A5)$$

$$\cong V \cos \Lambda \qquad (A5a)$$

so that, for small deflections, equation (A1) can be expressed as follows:

$$l = (\varphi - \Gamma \tan \Lambda) \, m_e \frac{\rho}{2} V^2 \cos^2 \Lambda c \qquad (A6)$$

The moment of this force about the elastic axis is assumed to be given by the product $l e_1 c$. The presence of a moment at zero lift due to camber will not affect the results in any manner, since the divergence speed depends only on the rates at which the aerodynamic and structural forces increase with the deformations.

Differential Equations

The differential equations of bending and torsion of the wing referred to the elastic axis are

$$\frac{d^2}{dy^2}\left(EI \frac{d\Gamma}{dy}\right) = l \qquad (A7)$$

$$\frac{d}{dy}\left(GJ \frac{d\varphi}{dy}\right) = -l e_1 c \qquad (A8)$$

respectively. Substituting the small-deflection expression for l (equation (A6)) into equations (A7) and (A8) yields the two simultaneous differential equations:

$$\frac{d^2}{dy^2}\left(EI \frac{d\Gamma}{dy}\right) = \frac{\rho}{2}V^2 \cos^2\Lambda m_e c \, (\varphi - \Gamma \tan \Lambda) \qquad (A9)$$

$$\frac{d}{dy}\left(GJ \frac{d\varphi}{dy}\right) = -\frac{\rho}{2}V^2 \cos^2\Lambda m_e e_1 c^2 \, (\varphi - \Gamma \tan \Lambda) \qquad (A10)$$

These equations are subject to the following boundary conditions:

Zero local dihedral and twist at the root,

$$\Gamma(0) = 0 \qquad (A11)$$

$$\varphi(0) = 0 \qquad (A11a)$$

Zero moment, torque, and shear at the free end,

$$\left(EI \frac{d\Gamma}{dy}\right)_{y=L} = 0 \tag{A12}$$

$$\left(GJ \frac{d\varphi}{dy}\right)_{y=L} = 0 \tag{A12a}$$

$$\left(EI \frac{d^2\Gamma}{dy^2}\right)_{y=L} = 0 \tag{A12b}$$

Equations (A9) and (A10) may be solved by numerical methods for any arbitrary stiffness and chord variation. In the case of untapered wings and linearly tapered wings with the stiffnesses varying as the chord to the fourth power, they can be solved directly, as shown in the following sections.

Solution for Uniform Wings

If the bending stiffness, the torsional stiffness, and the chord of the wing have constant values of $(EI)_r$, $(GJ)_r$, and c_r, respectively, along the wing span, equations (A9) and (A10) become

$$\Gamma''' \tan \Lambda = d(\varphi - \Gamma \tan \Lambda) \tag{A13}$$

$$\varphi'' = -a(\varphi - \Gamma \tan \Lambda) \tag{A14}$$

where the differentiation denoted by the prime is with respect to $\eta = \frac{y}{L}$ and the two dimensionless parameters a and d are defined by

$$a = \frac{q \cos^2\Lambda m_{e1} c_r^2 L^2}{(GJ)_r} \tag{A15}$$

$$d = \frac{q \cos^2\Lambda m_e c_r L^3 \tan \Lambda}{(EI)_r} \tag{A16}$$

Differentiating equation (A14) once and combining it with equation (A13) yields the single differential equation

$$\alpha_e''' + a\alpha_e' + d\alpha_e = 0 \tag{A17}$$

where $\alpha_e = \varphi - \Gamma \tan \Lambda$.

The general solution of this equation is

$$\alpha_e = \sum_{i=1}^{3} A_i e^{r_i \eta} \qquad (A18)$$

where the r_i's are the roots of the characteristic equation

$$r^3 + ar + d = 0 \qquad (A19)$$

and the A_i's are arbitrary constants.

The boundary conditions for equation (A17) are:

From equations (A11) and (A11a)

$$\alpha_e(0) = 0 \qquad (A20)$$

From equations (A12) and (A12a)

$$\alpha_e'(1) = 0 \qquad (A20a)$$

From equations (A14) and (A12b)

$$\alpha_e''(1) + a\alpha_e(1) = 0 \qquad (A20b)$$

Substituting equation (A18) into these boundary conditions gives

$$\left. \begin{array}{c} \displaystyle\sum_{i=1}^{3} A_i = 0 \\[3mm] \displaystyle\sum_{i=1}^{3} r_i A_i e^{r_i} = 0 \\[3mm] \displaystyle\sum_{i=1}^{3} (r_i^2 + a)A_i e^{r_i} = 0 \end{array} \right\} \qquad (A21)$$

The condition for divergence is that there be a nonvanishing solution for the A_i's; that is, a solution for which α_e is not zero along the entire span. Therefore, one or more of the A_i's must be different from zero (see equation (A18)). Hence, the determinant of the coefficients of the A_i's in equations (A21) must vanish. Thus,

$$\begin{vmatrix} 1 & 1 & 1 \\ r_1 e^{r_1} & r_2 e^{r_2} & r_3 e^{r_3} \\ \left(r_1{}^2 + a\right)e^{r_1} & \left(r_2{}^2 + a\right)e^{r_2} & \left(r_3{}^2 + a\right)e^{r_3} \end{vmatrix} = 0 \qquad \text{(A22)}$$

Critical combinations a_D and d_D of the parameters a and d are obtained if the combinations give rise to roots r_1, r_2, and r_3 for equation (A19) such that equation (A22) or its expanded equivalent is satisfied. The curve of a_D against d_D in figure 2 constitutes a plot of these critical combinations; points on the curve were computed by assuming values of a_D and solving for d_D by trial.

Solution for Tapered Wings

For tapered wings the chord varies linearly and the bending and torsion stiffnesses are assumed to vary as the fourth power of the chord. Then,

$$c = kc_r$$

where

$$k = 1 - (1 - \lambda)\eta$$

and λ is the taper ratio c_t/c_r. Furthermore,

$$GJ = (GJ)_r k^4$$

$$EI = (EI)_r k^4$$

The differential equations (A9) and (A10) then become

$$\tan \Lambda \left[k^3 \Gamma''' + 8k^2 \Gamma'' + 12k\Gamma' - d_T\Gamma\right] + d_T\varphi = 0 \qquad \text{(A23)}$$

$$\left[k^2 \varphi'' + 4k\varphi' + a_T\varphi\right] - a_T\Gamma \tan \Lambda = 0 \qquad \text{(A24)}$$

where

$$a_T = \frac{a}{(1 - \lambda)^2}$$

$$d_T = \frac{d}{(1 - \lambda)^3}$$

The differentiations denoted by the primes in equations (A23) and (A24) are with respect to k rather than η. This procedure places the differential equations in the form of the Euler (or Cauchy) equations, which are easily tractable mathematically.

Differentiating equation (A24) once, multiplying it by k, and combining the result with equations (A23) and (A24) yields a single differential equation in α_e:

$$k^3\alpha_e''' + 8k^2\alpha_e'' + (12 + a_T)k\alpha_e' + (2a_T - d_T)\alpha_e = 0 \qquad \text{(A25)}$$

The solution of this equation is

$$\alpha_e = \sum_{i=1}^{3} B_i k^{s_i} \qquad \text{(A26)}$$

where the s_i's are the roots of

$$s(s - 1)(s - 2) + 8s(s - 1) + (12 + a_T)s + (2a_T - d_T) = 0$$

or

$$s^3 + 5s^2 + (6 + a_T)s + (2a_T - d_T) = 0 \qquad \text{(A27)}$$

and the B_i's are arbitrary constants.

The boundary conditions are:

From equations (A11) and (A11a)

$$\alpha_e(1) = 0 \qquad \text{(A28)}$$

From equations (A12) and (A12a)

$$\alpha_e'(\lambda) = 0 \qquad \text{(A28a)}$$

From equations (A24), (A12a) and (A12b)

$$\lambda^2\alpha_e''(\lambda) + a_T\alpha_e(\lambda) = 0 \qquad \text{(A28b)}$$

Substituting equation (A26) into the boundary conditions gives

$$\left.\begin{array}{l} \displaystyle\sum_{i=1}^{3} B_i = 0 \\[2em] \displaystyle\sum_{i=1}^{3} s_i B_i \lambda^{s_i} = 0 \\[2em] \displaystyle\sum_{i=1}^{3} \left[s_i(s_i - 1) + a_T \right] B_i \lambda^{s_i} = 0 \end{array}\right\} \qquad \text{(A29)}$$

20

Setting the determinant of the coefficients of the B_i's in equation (A29) equal to zero yields, after some simplification,

$$
\begin{vmatrix}
1 & 1 & 1 \\
s_1\lambda^{s_1} & s_2\lambda^{s_2} & s_3\lambda^{s_3} \\
\left(s_1^2 + a_T\right)\lambda^{s_1} & \left(s_2^2 + a_T\right)\lambda^{s_2} & \left(s_3^2 + a_T\right)\lambda^{s_3}
\end{vmatrix} = 0
\qquad (A30)
$$

Equation (A30) is very similar to the corresponding determinantal equation (A22) for untapered wings. For particular values of the taper ratio λ, it determines critical combinations of a and d. Calculations have been carried out for taper ratios of 0.2, 0.5, and 1.5, and the results are given by the curves of a_D against d_D/a_D and d_D against a_D/d_D in figures 4(a), 4(b), and 4(c), together with the results of the analysis for the uniform wing (taper ratio 1.0).

REFERENCES

1. Reissner, H.: Neuere Probleme aus der Flugzeugstatik. Z.F.M., Jahrg. 17, Heft 7, April 14, 1926, pp. 137–146; Jahrg. 17, Heft 9, May 14, 1926, pp. 179–185; Jahrg. 17, Heft 18, Sept. 23, 1926, pp. 384–393, and Jahrg 18, Heft 7, April 14, 1927, pp. 153–158.

2. Shornick, Louis H.: The Computation of the Critical Speeds of Aileron Reversal, Wing Torsional Divergence and Wing–Aileron Divergence. MR No. ENG–M–51/VF18, Addendum 1, Materiel Center, Army Air Forces, Dec. 19, 1942.

3. Hildebrand, Frances B., and Reissner, Eric.: The Influence of the Aerodynamic Span Effect on the Magnitude of the Torsional– Divergence Velocity and on the Shape of the Corresponding Deflection Mode. NACA TN No. 926, 1944.

4. Pugsley, A. G., and Naylor, G. A.: The Divergence Speed of an Elastic Wing. R. & M. No. 1815, British A.R.C., 1937.

5. Fettis, Henry E.: Calculations of the Flutter Characteristics of Swept Wings at Subsonic Speeds. MR No. TSEAC5–4595–2–9, Air Materiel Command, Army Air Forces, May 13, 1946.

6. Toll, Thomas A., and Queijo, Manuel J.: Approximate Relations and Charts for Low–Speed Stability Derivatives of Swept Wings. NACA TN No. 1581, 1948.

7. Zender, George, and Libove, Charles: Stress and Distortion Measurements in a 45° Swept Box Beam Subjected to Bending and to Torsion. NACA TN No. 1525, 1948.

TABLE I.— RESULTS OF DIVERGENCE TESTS

$-\Lambda$ (deg)	q_D (experiment) (lb/sq ft)	q_D (calculated) (lb/sq ft)	
Series 1			
5 in. by 30 in. by 0.126 in.; square tips; $e_1 = 0.25$; $(GJ)_r = 13{,}330$ lb–in.^{2}; $(EI)_r = 8{,}830$ lb–in.^{2}			
0	[a]112.80	178.6	
5.0	83.20	80.7	
14.7	44.21	40.9	
30.0	26.50	27.0	
45.0	24.41	26.2	
55.9	24.84	31.1	
55.9	24.95	31.1	
63.2	26.65	39.7	
Series 2			
4 in. by 24 in. by 0.0977 in.; square tips; $e_1 = 0.25$; $(GJ)_r = 4{,}980$ lb–in.^{2}; $(EI)_r = 3{,}300$ lb–in.^{2}			
0	[a]106.90	163.1	
5.0	76.99	73.8	
14.7	43.10	37.4	
30.0	26.51	24.7	
45.0	22.44	23.8	
60.0	23.36	32.0	
69.6	23.74	50.5	
Series 3			
5 in. by 30 in. by 0.125 in.; tips parallel to plane of symmetry; $e_1 = 0.25$; $(GJ)_r = 13{,}050$ lb–in.^{2}; $(EI)_r = 8{,}560$ lb–in.^{2}			
		Root A	Root B
5.6	79.87	74.0	74.8
15.5	41.80	38.3	40.8
30.1	31.72	26.5	30.3
45.2	28.90	25.3	32.8
[b]59.7	[c]38.18	33.7	53.1
74.6	54.62	79.3	232.4

[a]Flutter.
[b]Model thickness, 0.123 inch.
[c]Corrected for discrepency in thickness.

NACA
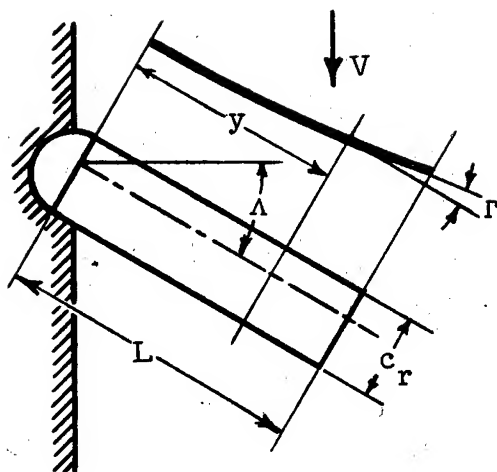
(a) Assumed constant-chord wing.
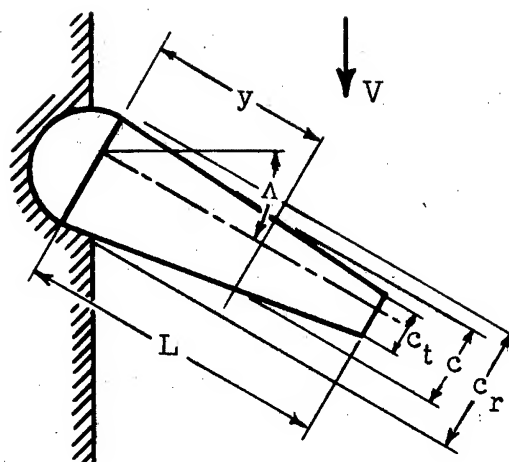
(b) Assumed tapered wing.
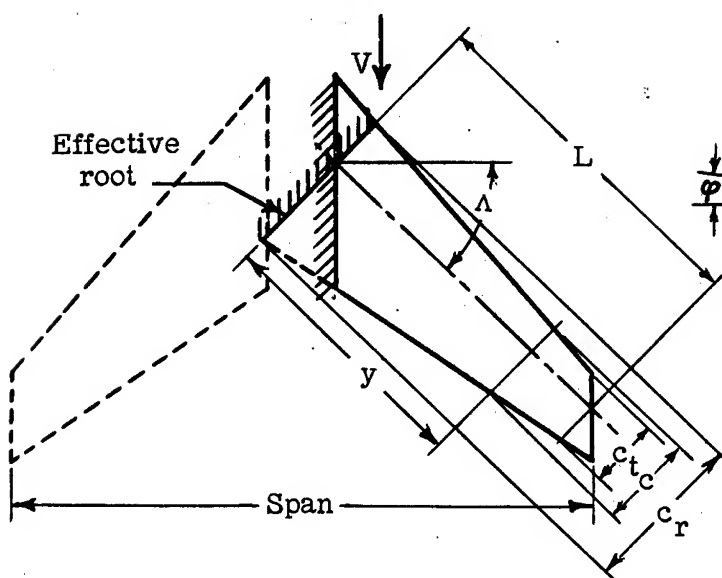
(c) Actual wing.
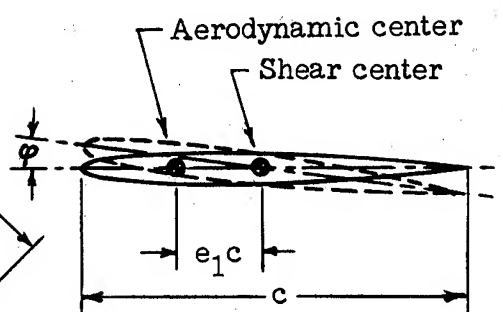
Elastic axis

Figure 1.- Definitions of geometrical parameters.
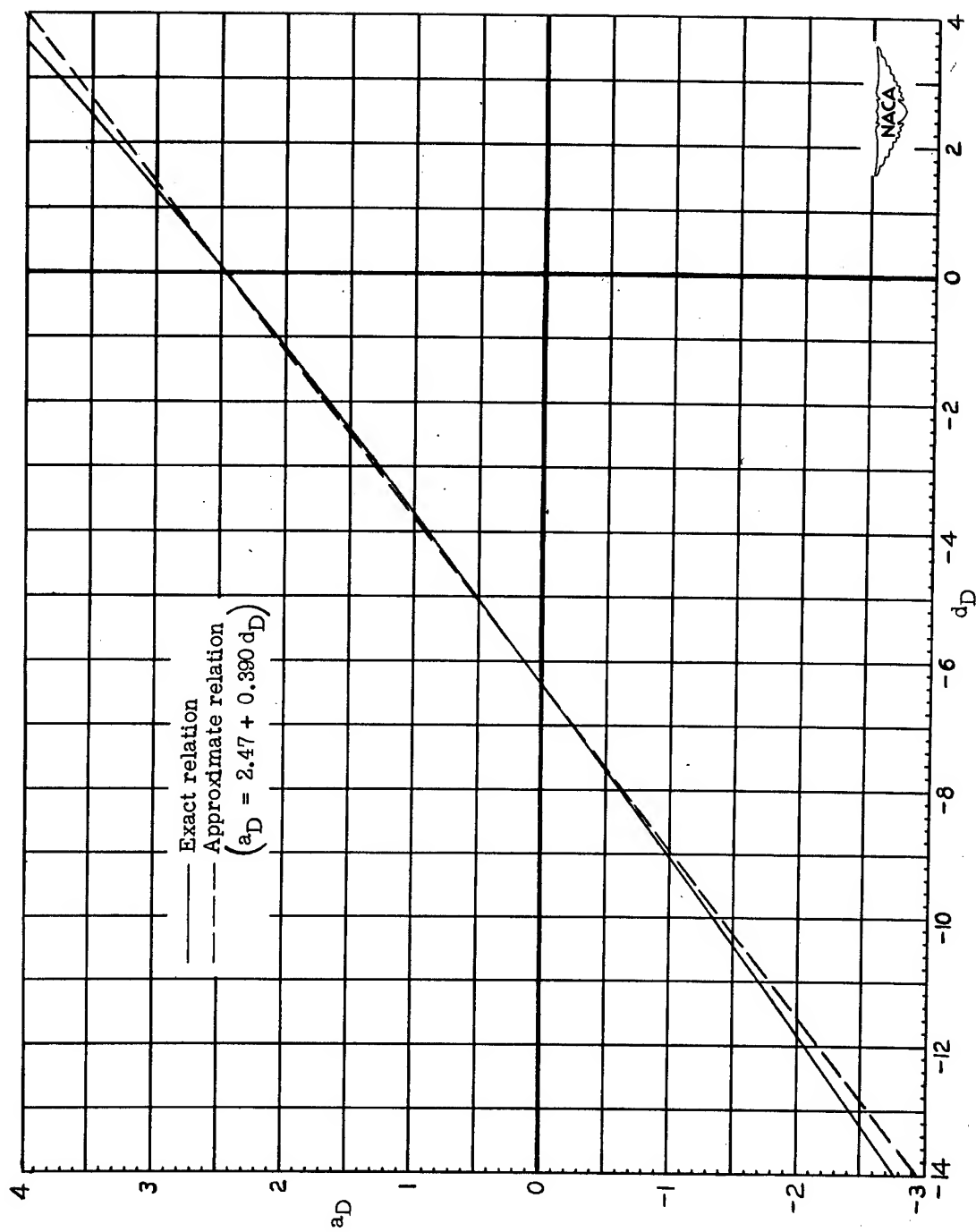
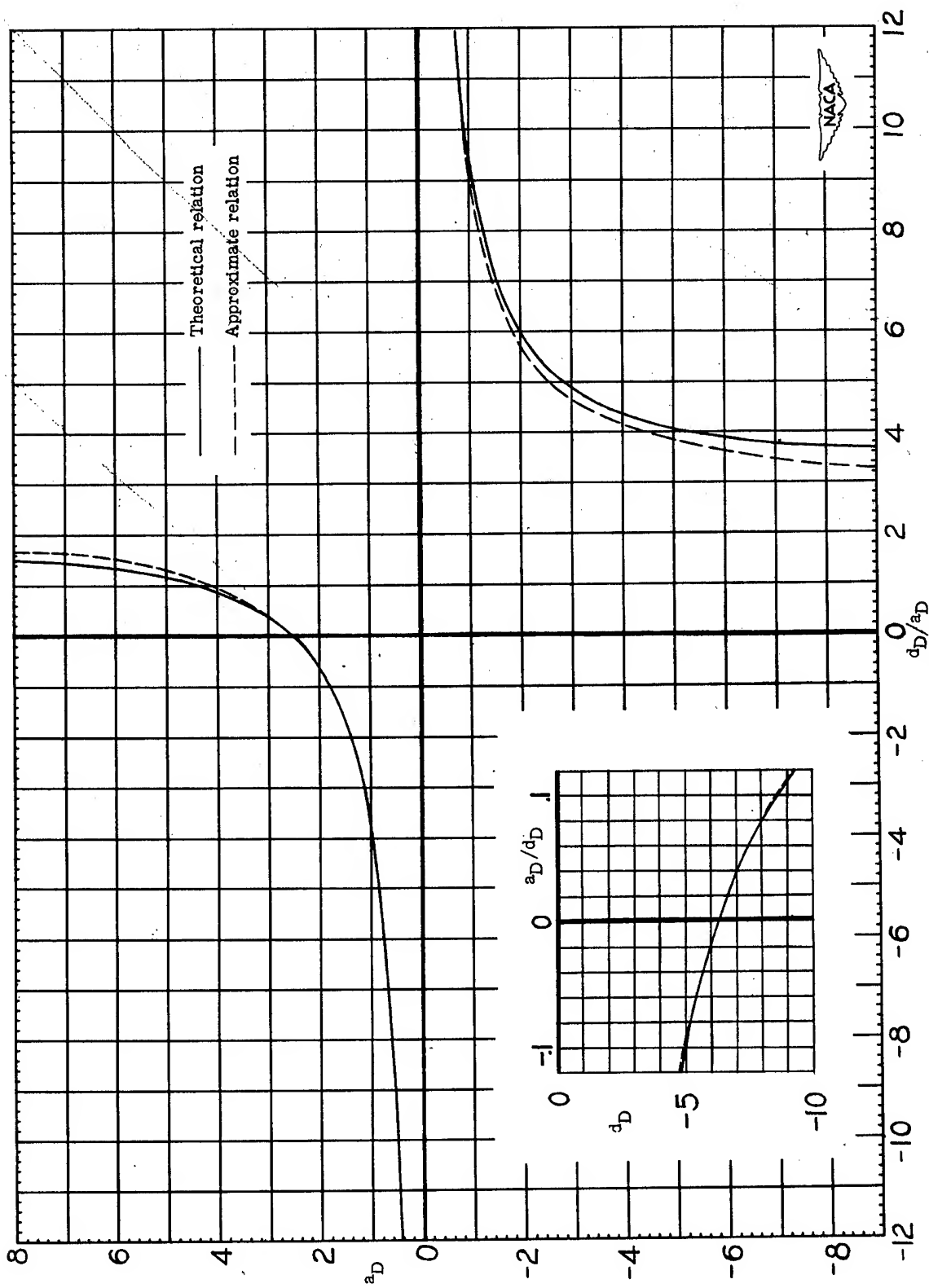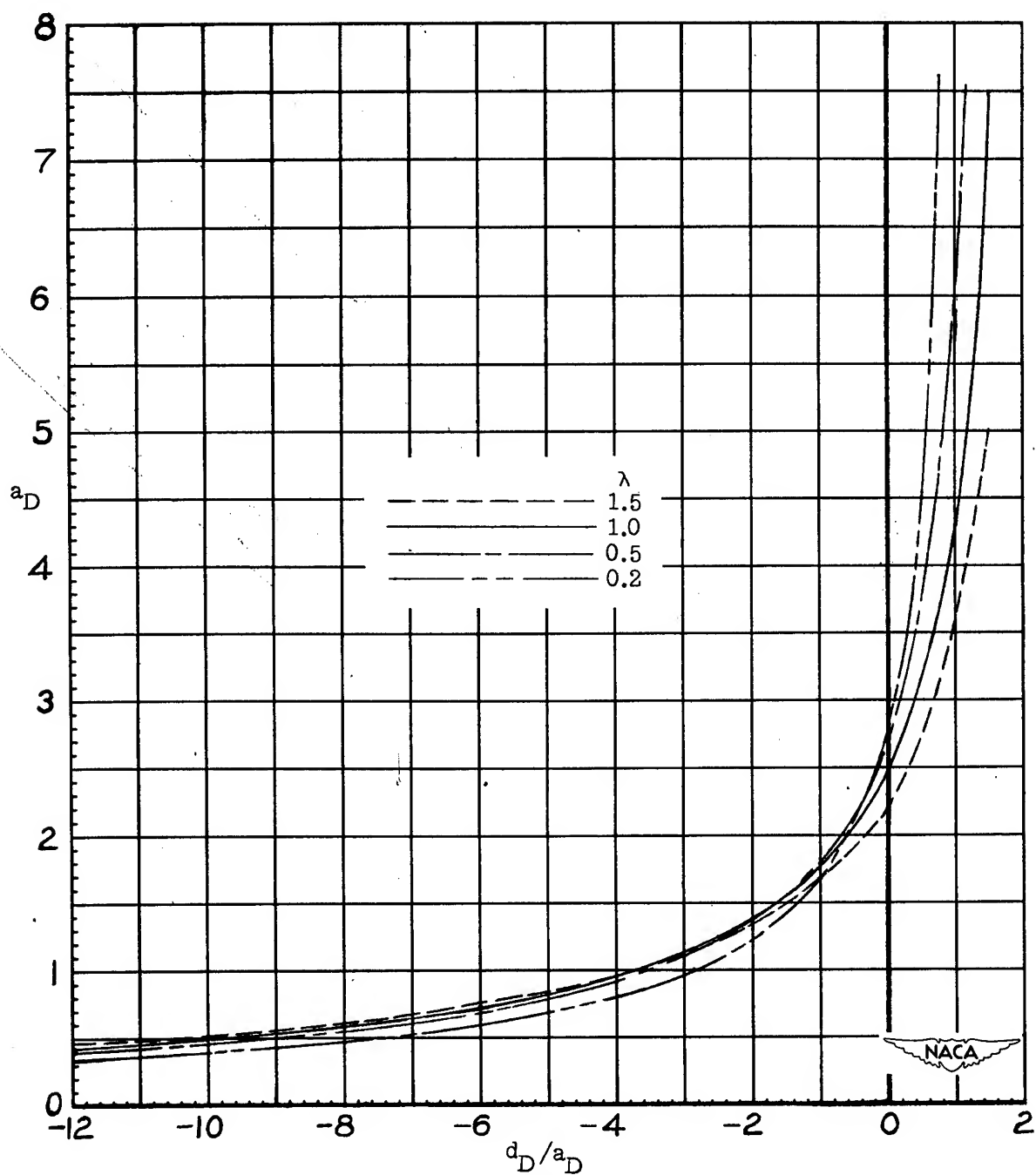Figure 2.- The relation between the parameters a_D and d_D. Uniform wing.

Exact relation
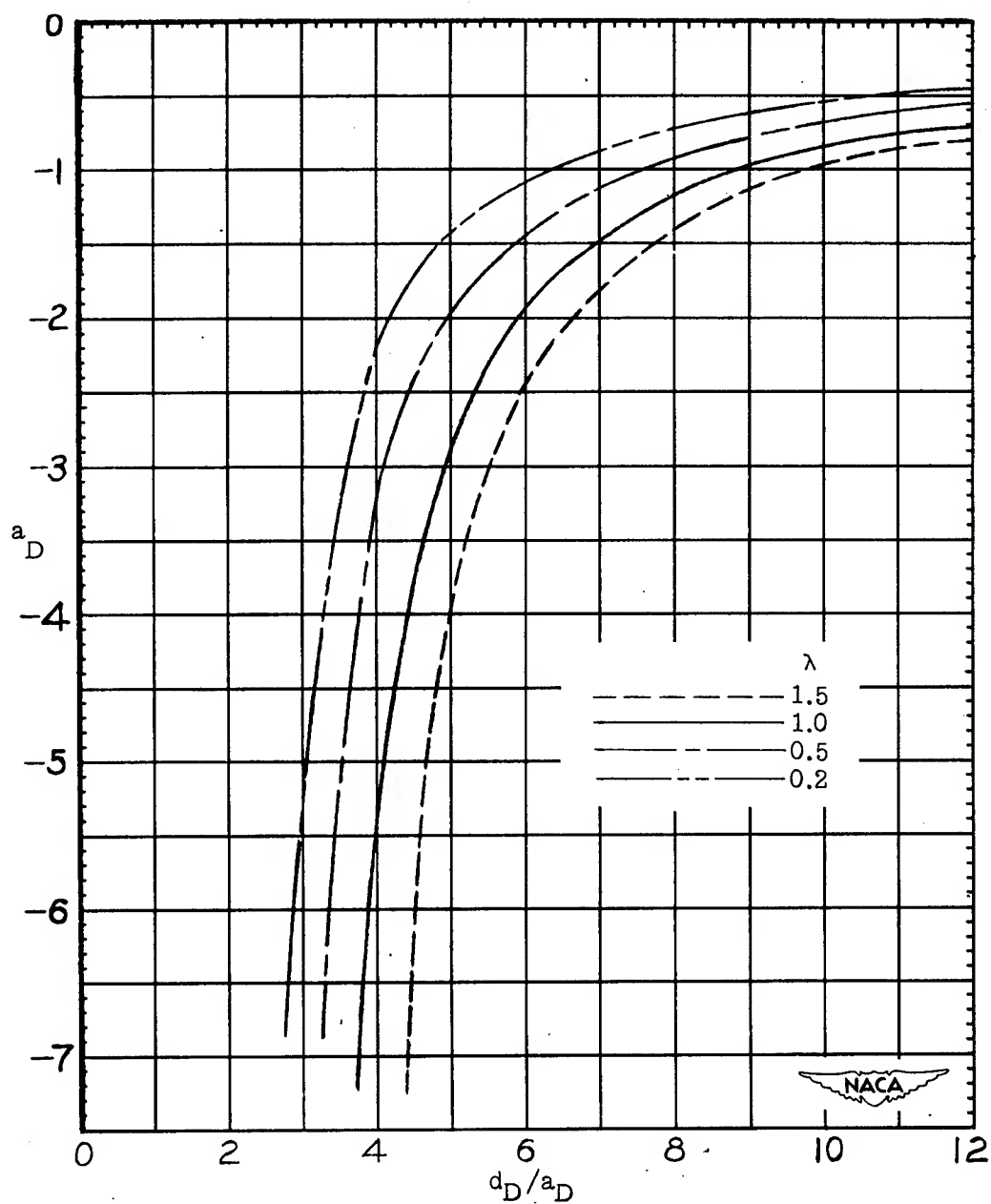Approximate relation
$\left(a_D = 2.47 + 0.390 \, d_D\right)$

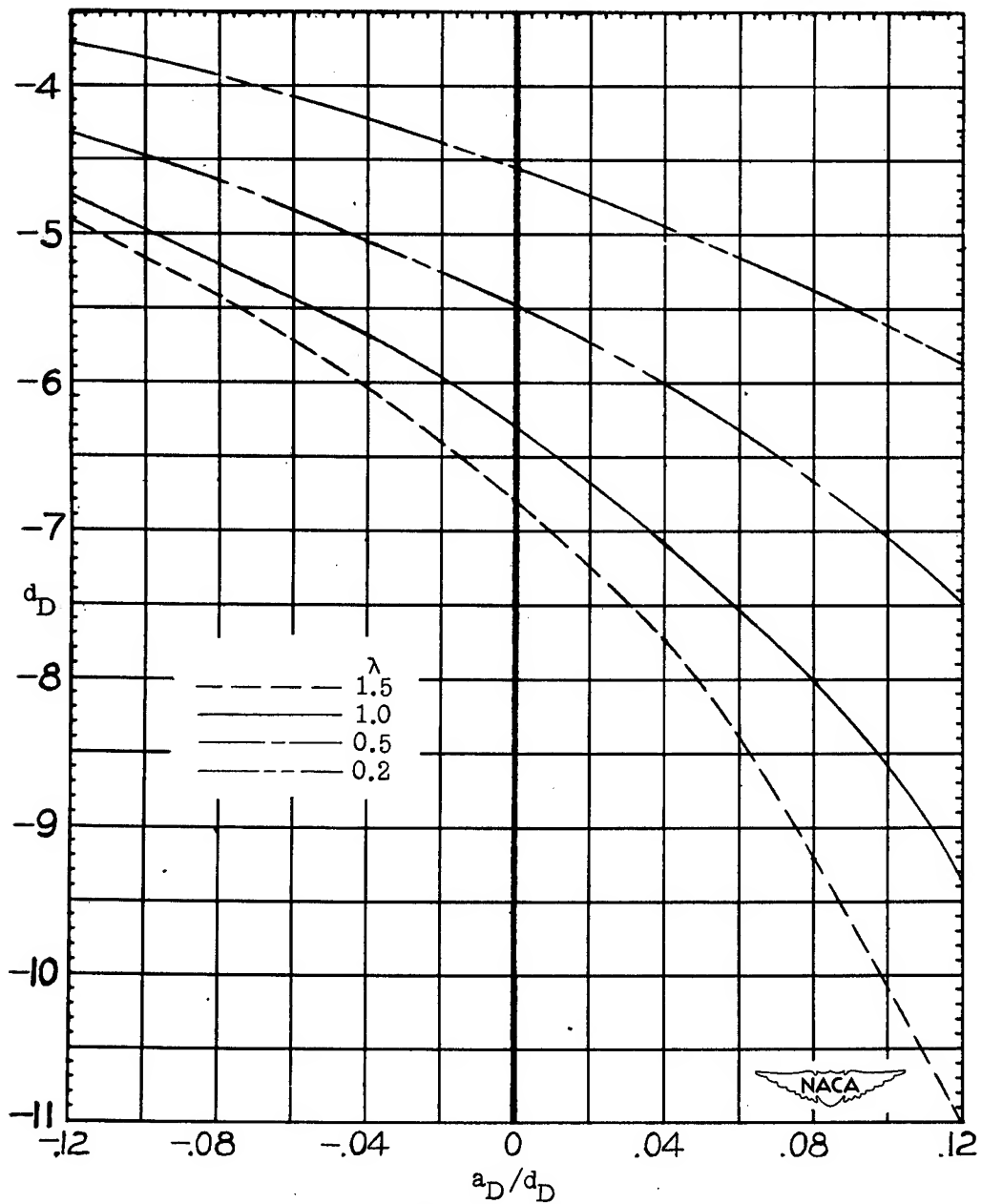Figure 3.- The relation between the parameters a and d at divergence for a uniform wing.

(a) Negative values of d_D/a_D .

Figure 4.- Divergence of swept wings.

(b)   Positive values of d_D/a_D.

Figure 4.- Continued.

(c) Large values of d_D/a_D.

Figure 4.- Concluded.
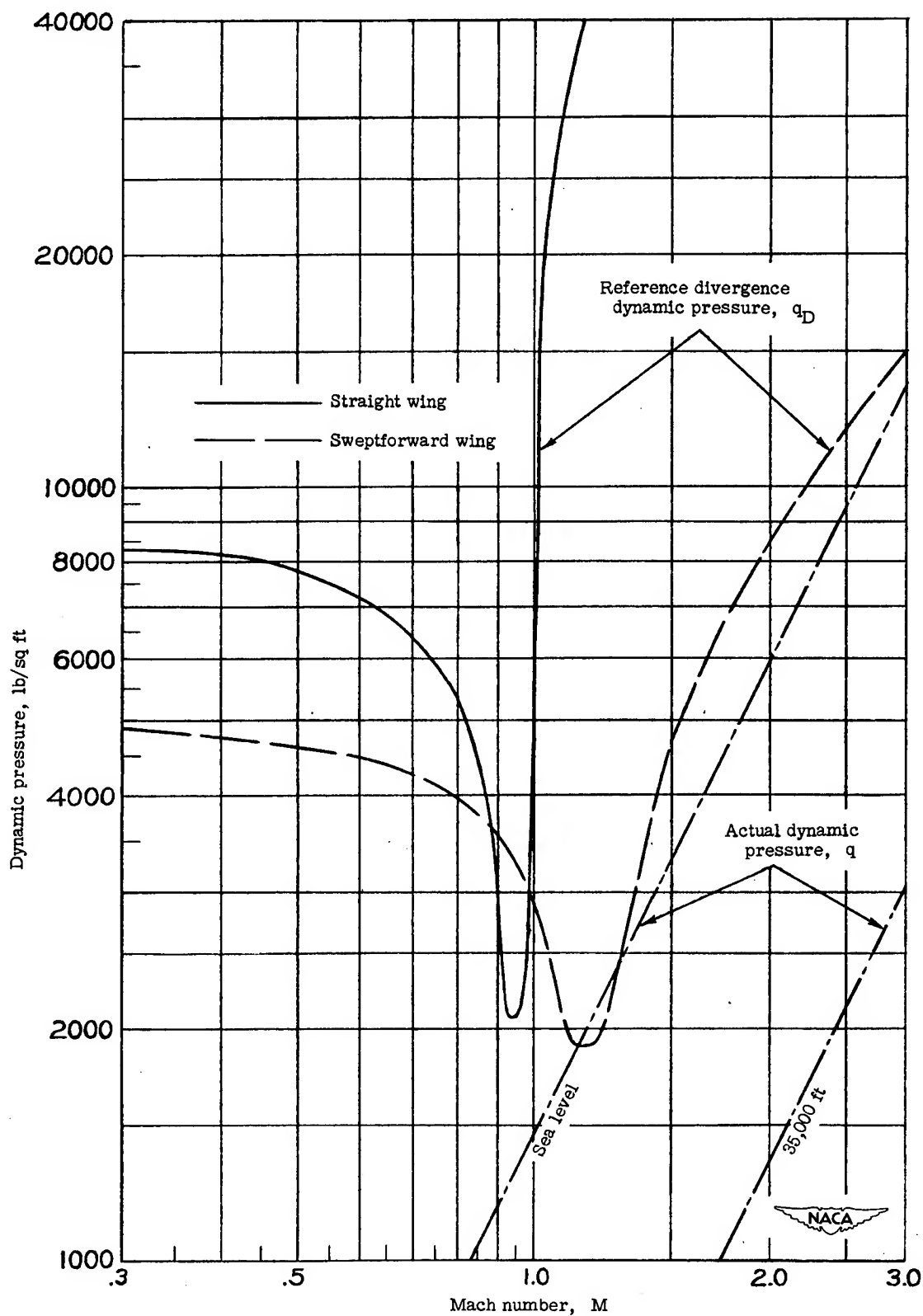
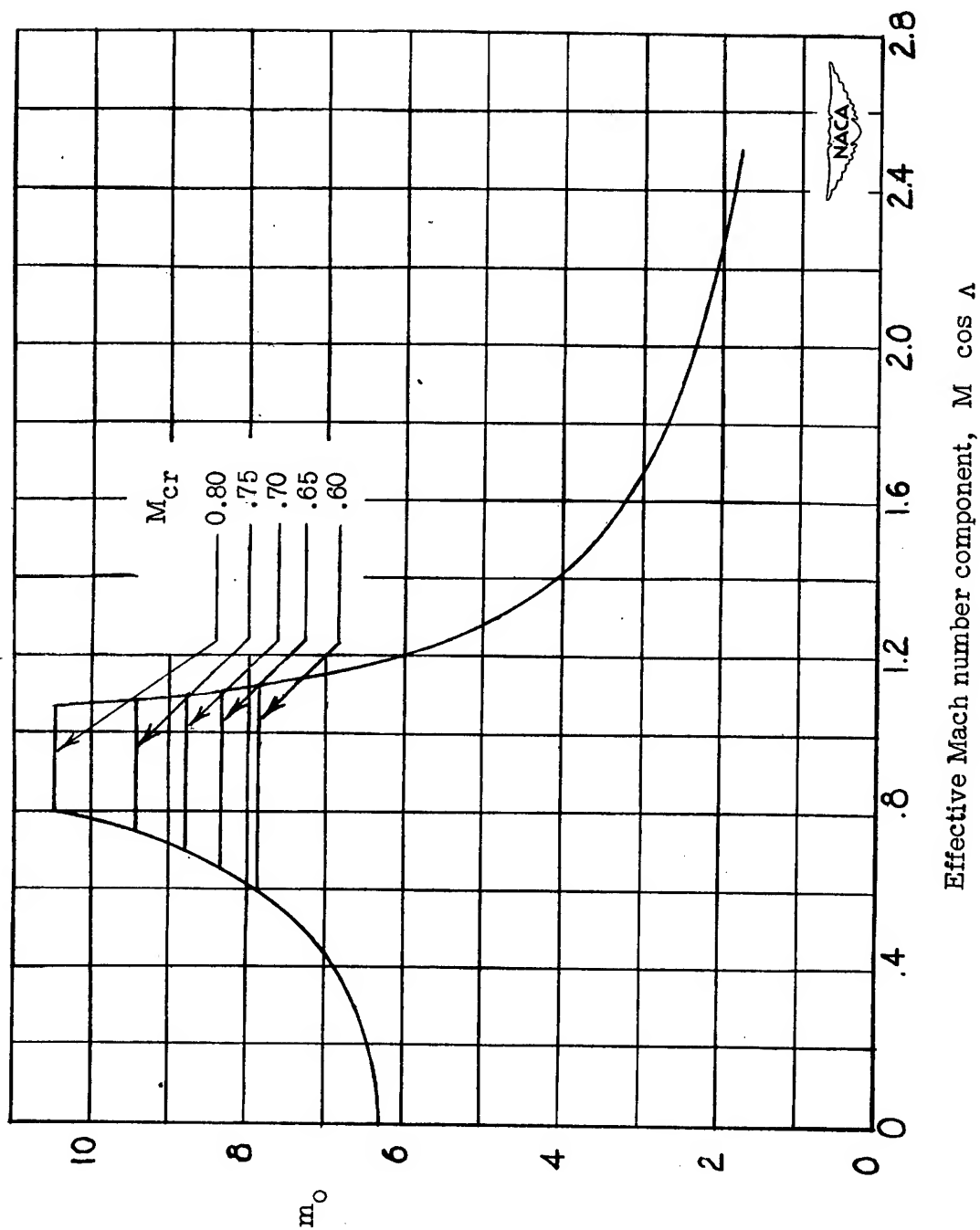Figure 5.- Divergence of a straight and a sweptforward wing.

Effective Mach number component, $M \cos \Lambda$

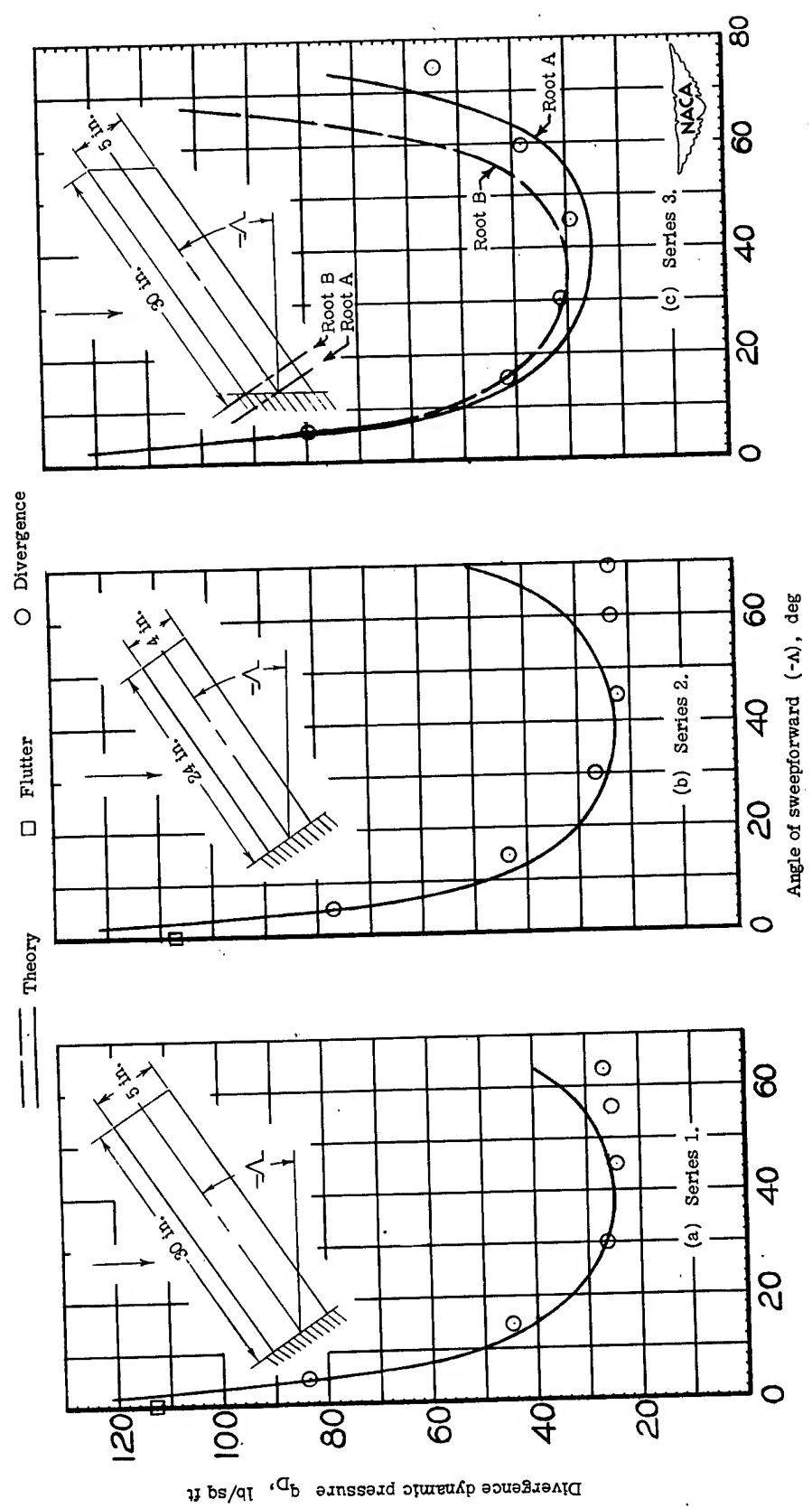Figure 6.- Approximate value of the section lift-curve slope m_o.

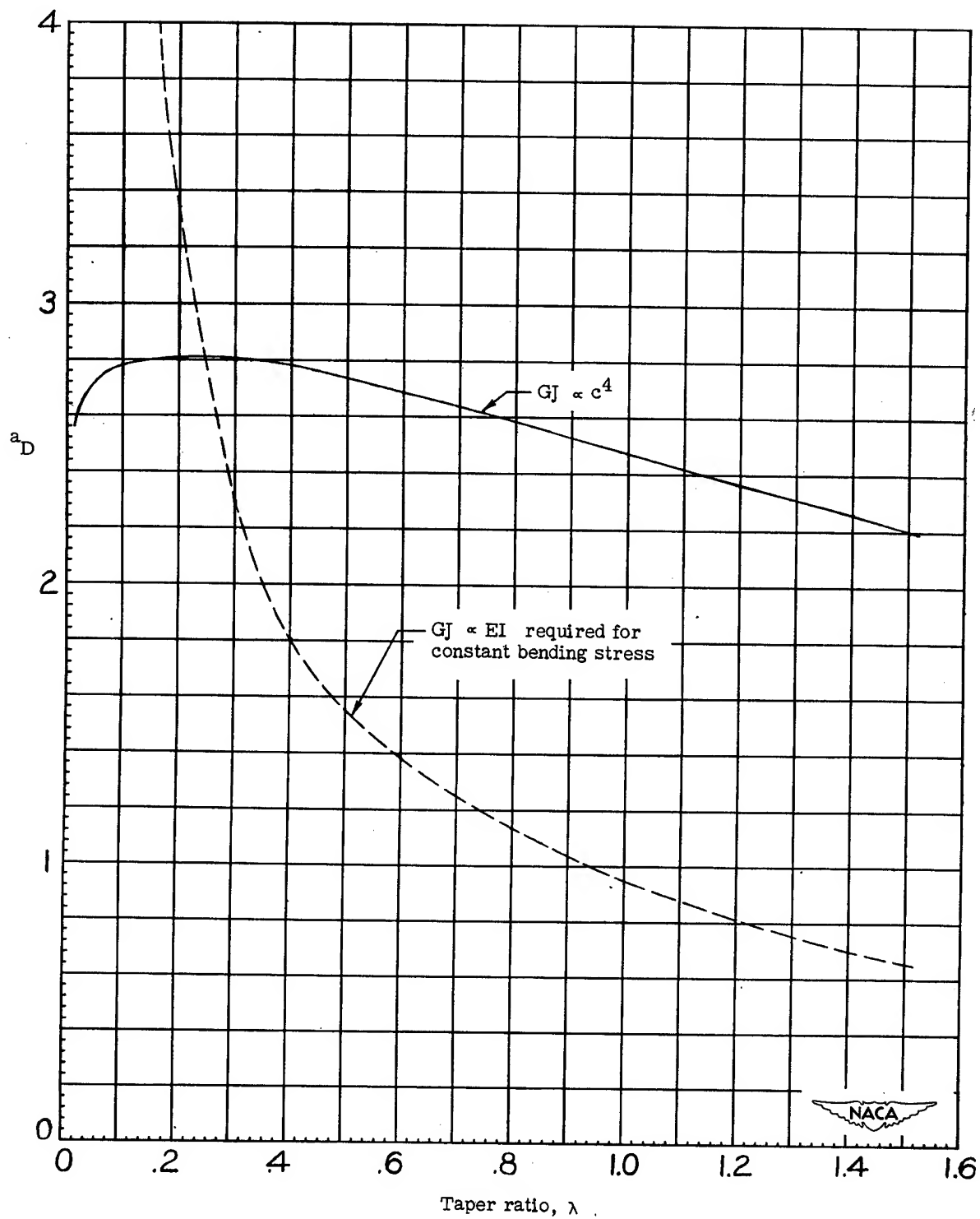Figure 7.- Experimental and theoretical results for the divergence of uniform swept wings.

Figure 8.- Effect of taper on the divergence of unswept wings.